Monthly Notices of the ROYAL ASTRONOMICAL SOCIETY

MNRAS **439,** 878–886 (2014) doi:10.1093/mnras/stu010
Advance Access publication 2014 February 4

Dynamical analyses of the companions orbiting eclipsing binaries – I. SW Lacertae

Jinzhao Yuan[1]★ and Hakan Volkan Şenavcı[2]

[1]*Department of Physics, Shanxi Normal University, Linfen 041004, Shanxi, China*
[2]*Department of Astronomy and Space Sciences, Ankara University, Faculty of Science, TR-06100 Tandoğan-Ankara, Turkey*

Accepted 2014 January 2. Received 2013 December 31; in original form 2013 October 6

ABSTRACT

New mid-eclipse times of the short-period eclipsing binary SW Lacertae are reported, and two cyclical variations are found in the corresponding $O - C$ diagram. The proposed light-travel time model is refined. The best fit suggests that two possible circumbinary companions are in a near 3:1 mean-motion resonance with periods of 27.01 and 82.61 yr. Based on the best-fitting solution, we have studied the stabilities of the two companions moving on a series of mutually inclined orbits. The results show that no orbital configurations can survive for >1000 yr. Then, non-Keplerian corrections to the initial conditions and the more distant K-dwarf companion discovered by Ruciński, Pribulla & van Kerkwijk, moving on assumed circular orbits with wide ranges of orbital inclinations, are considered in our numerical simulations. The outcome similarly reveals that the whole system is yet short-term unstable. Perhaps, one or both cyclical variations in the mid-eclipse times are attributed to irregular mass exchange and/or magnetic cycles in the magnetically active W UMa system. Despite this, the instability of the system may also arise from the large uncertainties in orbital parameters. So, secular observations of this target are needed to determine the eccentricity of the outmost companion and the orbital period of the middle companion with much higher precision. Our results suggest that, if the two inner companions do exist, they should be on mutually inclined orbits of >100°, with the minimum masses of 0.62 and 1.94 $M_\odot$ for the innermost and middle components, respectively. Our work demonstrates that it is important and necessary to perform dynamical analyses before a discovery of two or more circumbinary companions is announced.

Key words: methods: numerical – binaries: close – binaries: eclipsing – stars: individual: SW Lacertae.

1 INTRODUCTION

SW Lacertae (hereafter SW Lac AB) is a well-known contact binary for its short period, high brightness and variable light curves. The light curves have been analysed by Zhai & Lu (1989), Al-Naimiy & Al-Masharfeh (2000), Albayrak et al. (2004) and more recently by Alton & Terrell (2006). The former has also derived spectroscopic mass ratio of $q = 0.797 \pm 0.010$ from radial velocity curves, compared to $q = 0.776 \pm 0.012$ presented by Ruciński et al. (2005). Şenavcı et al. (2011) performed Doppler mapping of the system, and concluded that the spot coverage is 2 per cent for the primary component and 3 per cent for the secondary component. A late-type tertiary component was discovered in the spectroscopic observation by Hendry & Mochnacki (1998) and contributes about 1 per cent of the total light (Ruciński et al. 2005).

The observed period has been analysed for several times since Dugan & Wright (1939) found its complex variability. Panchatsaram & Abhyankar (1981) used two sinusoidal curves to fit the $O - C$ values and interpreted them as light-travel time (LTT) effect caused by the orbital motion of two circumbinary companions (hereafter, referred to as SW Lac C and D). The latest analysis was performed by Pribulla, Chochol & Parimucha (1999), who found another quadratically variable component. However, many mid-eclipse times have been obtained in the past 14 yr. It is necessary to re-analyse the behaviour of the change in the observed period.

2 THE DATABASE

We carried out the CCD observations of SW Lac in three consecutive years (2010–2012) using the 85 cm telescope at the Xinglong Station of National Astronomical Observatory of China (NAOC85),

★ E-mail: yuanjz@sxnu.edu.cn

© 2014 The Authors
Published by Oxford University Press on behalf of the Royal Astronomical Society

Downloaded from https://academic.oup.com/mnras/article/439/1/878/1747721 by ANKARA user on 12 December 2021

Table 1. Several new mid-eclipse times of SW Lac.

HJD (UTC) 240 0000+	BJD (TDB) 240 0000+	Errors (d)	Min.	Filters	$O-C$ (d)	Origin
555 30.937 73	555 30.938 48	±0.000 05	I	*V*	−0.021 91	NAOC85
558 37.386 13	558 37.386 88	±0.000 05	II	*BVR*	−0.019 84	AUKR-T40
558 37.547 65	558 37.548 40	±0.000 06	I	*BVR*	−0.018 68	AUKR-T40
558 38.348 22	558 38.348 97	±0.000 05	II	*BVR*	−0.019 91	AUKR-T40
558 38.510 00	558 38.510 75	±0.000 06	I	*BVR*	−0.018 49	AUKR-T40
561 81.362 66	561 81.363 43	±0.000 02	I	*BVR*	−0.013 67	AUKR-T40
561 81.522 55	561 81.523 32	±0.000 05	II	*BVR*	−0.014 14	AUKR-T40
561 82.324 80	561 82.325 57	±0.000 04	I	*BVR*	−0.013 68	AUKR-T40
561 82.484 66	561 82.485 43	±0.000 04	II	*BVR*	−0.014 18	AUKR-T40
562 39.093 13	562 39.093 90	±0.000 05	I	*V*	−0.012 87	NAOC85
562 40.055 27	562 40.056 04	±0.000 02	I	*V*	−0.012 88	NAOC85

equipped with a primary-focus multicolour CCD photometer (Zhou et al. 2009), and the 40 cm Schmidt–Cassegrain telescope at the Ankara University Kreiken Observatory of Turkey (AUKR-T40). The data reduction is performed by using the aperture photometry package IRAF[1] (biassubtraction, flat-field division). Extinction corrections are ignored as the comparison star is very close to the variable. In total, 11 new mid-eclipse times are obtained and listed in Table 1. A mean mid-eclipse time is given if multiband values are obtained.

In order to derive the parameters of companions around SW Lac, we collect all mid-eclipse times along with their errors in the literature. The complete photographic data are taken from Woodward (1951). Just as Pribulla et al. (1999) did, the photographic data later than the first photoelectric time obtained in 1951 October are rejected due to their relatively large errors. We collect 638 photoelectric and CCD mid-eclipse times mainly from Brownlee (1957), Kwee (1958), Broglia (1962), Widorn (1962), Chou (1963), Bookmyer (1965), Lang & Vetešník (1966), Pohl (1967), Kalchaev, Laytschev & Trutse (1968), Ruciński (1968), Pohl & Kızılırmak (1970, 1972), Muthsam & Rakos (1974), Kızılırmak & Pohl (1974), Aslan et al. (1981), Hopp, Hoffmann & Witzigmann (1982), Faulkner et al. (1984), Niarchos (1985), Evren, Akan & İbanoğlu (1985), Pohl et al. (1987), Mullis & Faulkner (1991), Essam, Mahdy & Hamdy (1992), BAV-M 50, Demircan et al. (1994), Müyesseroglu, Gürol & Selam (1996), BAV-M 59, Pribulla et al. (1999), Albayrak & Gürol (2001), Derekas, Kiss & Bebes (2002), Albayrak et al. (2004), Hübscher, Paschke & Walter (2006), Alton & Terrell (2006), Brát, Zejda & Svoboda (2007), Kılıçoğlu et al. (2007), Şenavcı et al. (2007) and Hübscher et al. (2010). If the mid-eclipse times were published without errors, a probable error of ±0.0003 d is assumed for the photoelectric and CCD data, and ±0.004 d for photographic and visual data. The error of ±0.0001 d is adopted if it is less than ±0.0001 d. A total of 766 mid-eclipse times, which have a coverage of 127 yr, are used in this paper.

To ensure uniform timing analysis, all Heliocentric Julian Dates (HJD) in Coordinated Universal Time (UTC) system have been converted to Barycentric Julian Dates (BJD) in Barycentric Dynamical Time (TDB) system using the UTC2BJD[2] procedure developed by Eastman, Siverd & Gaudi (2010).

[1] IRAF is developed by the National Optical Astronomy Observatories, which are operated by the Association of Universities for Research in Astronomy, Inc., under contract to the National Science Foundation.
[2] http://astroutils.astronomy.ohio-state.edu/time/

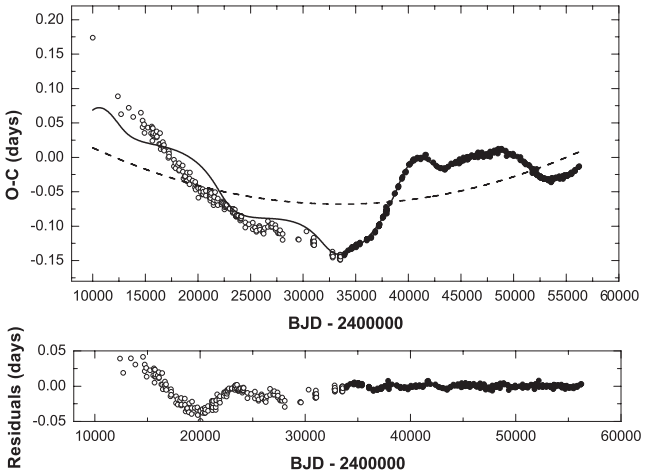


Figure 1. $O-C$ diagram of SW Lac. The filled circles refer to photoelectric and CCD data and open circles to photographic and visual observations. The solid line denotes the best fit with equation (2), and the dashed line only represents the quadratic part in the equation. Note that the error bars of the photoelectric and CCD data are smaller than the size of their dots, while the error bars of the photographic and visual data are not plotted since most of their errors are missing. The residuals from equation (2) are displayed in the lower panel.

The eclipse-timing residuals, $O-C$, are computed with respect to the ephemeris given by Kreiner, Kim & Nha (2000),

$$\text{Min } I = \text{BJD}243\,8708.3234 + 0^d.320\,7183 \times E, \quad (1)$$

and displayed in Fig. 1.

As mentioned before, Pribulla et al. (1999) used an ephemeris including a quadratic and two LTT terms (Irwin 1952) to fit the $O-C$ values:

$$O-C = C_0 + C_1 \times t + C_2 \times t^2 + \frac{a_3 \sin i_3}{c}\left[\frac{1-{e_3}^2}{1+e_3\cos\nu_3}\sin(\nu_3+\omega_3) + e_3\sin\omega_3\right] + \frac{a_4 \sin i_4}{c}\left[\frac{1-{e_4}^2}{1+e_4\cos\nu_4}\sin(\nu_4+\omega_4) + e_4\sin\omega_4\right], \quad (2)$$

where $a_3 \sin i_3$ is the projected semimajor axis of the binary pair around the barycentre of SW Lac AB and C (i_3 denotes the orbital inclination of inner companion with respect to the tangent plane of the sky), e_3 the eccentricity and c the speed of light. In equation (2), ω_3 is the argument of the periastron measured from the ascending

Downloaded from https://academic.oup.com/mnras/article/439/1/878/1747721 by ANKARA user on 12 December 2021

node in the tangent plane of the sky and v_3 the true anomaly, which is related with the mean anomaly of $M = 2\pi(t - T_3)/P_3$, where T_3 and P_3 are the time of the periastron passage and orbital period, respectively. All parameters with the subscript '4' are similar to those with the subscript '3', but refer to the barycentre of SW Lac AB and C around the barycentre of SW Lac AB, C and D. During the fitting process, 13 parameters have to be determined. In this paper, however, a two-dimensional Keplerian periodogram, which is similar to the generalized Lomb–Scargle (GLS) periodogram (Zechmeister & Kürster 2009), is developed. We write equation (2) as a linear equation:

$$O - C = C_0 + C_1 \times t + C_2 \times t^2 + \sum_{k=3,4} (A_k \cos E_k + B_k \sin E_k), \tag{3}$$

with the coefficients

$$A_k = \frac{a_k \sin i_k}{c} \cdot \sin \omega_k,$$

$$B_k = \sqrt{1 - e_k^2} \cdot \frac{a_k \sin i_k}{c} \cdot \cos \omega_k, \tag{4}$$

where E_k are the eccentric anomaly. Given one grid point in the space of the parametric set (e_3, T_3, P_3, e_4, T_4, P_4), the best-fitting values of the coefficients C_0, C_1, C_2, A_1, B_1, A_2 and B_2 can be derived by linear regression. This fitting process is to minimize the weighted sum of the squared difference between the $O - C$ values, y_i and the model value $y(t_i)$ at light minima times t_i:

$$\chi^2 = \sum_{i=1}^{N} \omega_i [y_i - y(t_i)]^2, \tag{5}$$

where

$$\omega_i = \frac{1}{{\sigma_i}^2} / \sum_{j=1}^{N} \frac{1}{{\sigma_j}^2} \tag{6}$$

are the normalized weights, σ_i the standard errors of the given individual data sets and N the number of observations. Scanning the whole parameter space yields the best Keplerian fit, which is listed in the second column (Solution 1) of Table 2. In Fig. 2, we plot the χ^2 contours for the best-fitting solution, including the two-dimensional Keplerian periodogram.

In order to improve the precision of the solutions, we need smaller grids, and therefore more computational time. Base on the GLS parameters, we adopt a non-linear least-squares algorithm, the Levenberg–Marquardt (LM) method, implemented in an IDL routine called MPFIT (Markwardt 2009). The true global minimum is found near the GLS parameters and gives orbital periods of 27.01 and 82.61 yr for these two companions, suggesting a near 3:1 mean-motion resonance (MMR). The result is summarized in the third column (Solution 2) of Table 2 and plotted in Fig. 1.

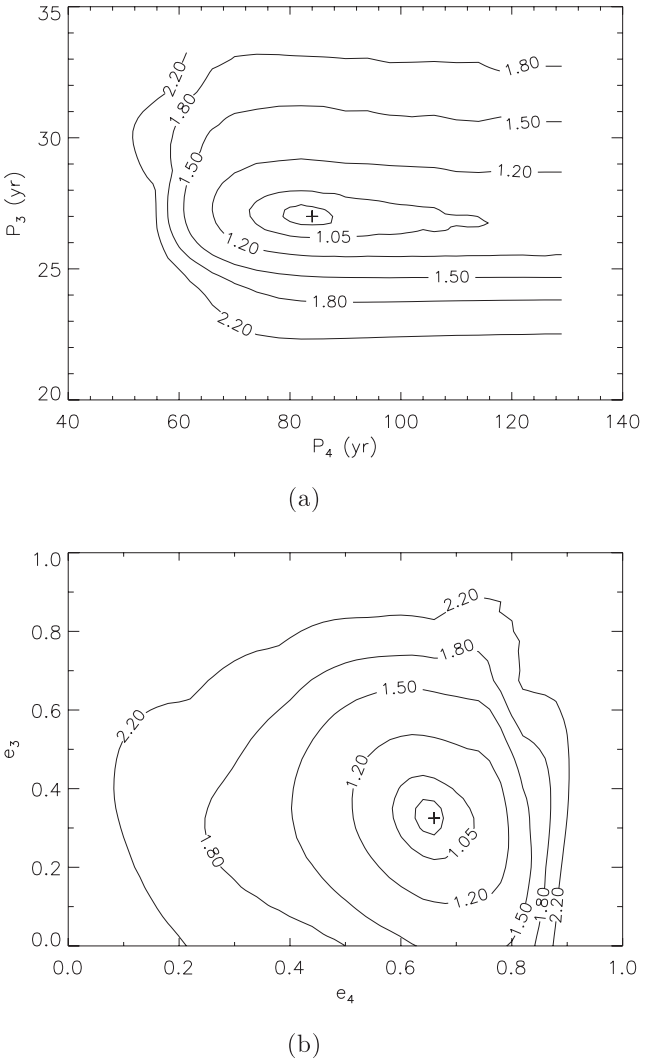


Figure 2. Two-dimensional constraints on orbital periods (a) and eccentricities (b). The χ^2 distributions are normalized by the χ^2 minimum, which is marked by the cross. The contours correspond to 1.01, 1.05, 1.20, 1.50, 1.80 and 2.20 times the χ^2 minimum.

Table 2. The best-fitting Keplerian parameters using the GLS algorithm and the LM algorithm. Formal errors were obtained from the covariance matrix.

Parameter	Solution 1 (GLS)	Solution 2 (LM)	Solution 3 (LM)	Solution 4 (LM)
P_3 (yr)	27.00±0.25	27.01±0.02		27.03±0.02
T_3 (BJD)	2412 528±183	2412 529±29		2412 499±28
e_3	0.325±0.25	0.329±0.002		0.331±0.002
$a_3 \sin i_3$ (au)	2.856 77	2.84±0.01		2.84±0.01
ω_3 (deg)	206.697	206.9±0.4		206.6±0.4
P_4 (yr)	84.0±2.0	82.61±0.29	47.15±0.01	81.0765(fixed)
T_4 (BJD)	2439 269±0.5	2439 235±5	2438 093±3	2439 226±5
e_4	0.66±0.02	0.649±0.001	0.650±0.001	0.644±0.001
$a_4 \sin i_4$ (au)	13.1162	12.91±0.03	6.58±0.01	12.72±0.02
ω_4 (deg)	10.9656	10.5±0.1	2.3±0.1	10.3±0.1
χ^2	3.78×10^{-6}	3.60×10^{-6}	2.36×10^{-5}	3.61×10^{-6}

Downloaded from https://academic.oup.com/mnras/article/439/1/878/1747721 by ANKARA user on 12 December 2021

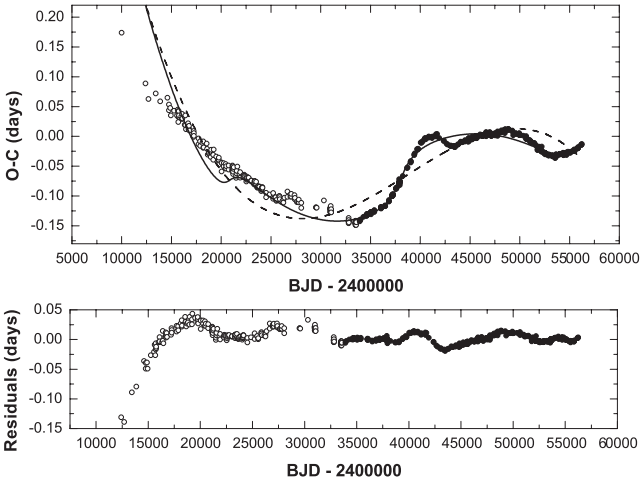


Figure 3. The same as in Fig. 1, but for the best fit with equation (7).

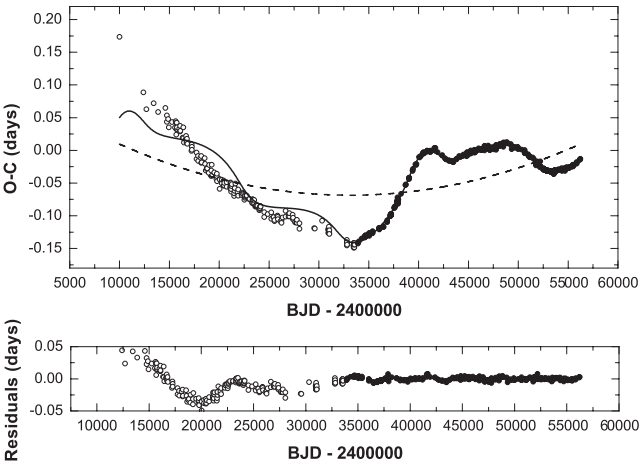


Figure 4. The same as in Fig. 1, but for the best fit with a strict 3:1 MMR model.

As shown in Fig. 1, the two-LTT ephemeris plus a quadratic trend has a good fit except for the points prior to BJD 242 5000 (i.e. 1927 April), where the cyclic variations with a period of 27.01 yr are unseen. Thus, we suspect that SW Lac C may not exist. Then, a single-LTT ephemeris plus a cubic trend

$$O-C = C_0 + C_1 \times t + C_2 \times t^2 + C_3 \times t^3 + \frac{a_4 \sin i_4}{c}\left[\frac{1-{e_4}^2}{1+e_4\cos\nu_4}\sin(\nu_4+\omega_4)+e_4\sin\omega_4\right] \quad (7)$$

is used to refit the $O-C$ data. The parameters derived from the best fit are listed in the fourth column (Solution 3) of Table 2, and the best fit is plotted in Fig. 3. The corresponding minimum χ^2 of 2.36×10^{-5} is much larger than that of Solution 2, suggesting that the cyclic variations with a period of $P_3 = 27.01$ yr do exist. Perhaps the cyclic variation is quasi-periodic. However, as mentioned before, the quadratic and two-LTT ephemerides fit the photoelectric and CCD data very well, throughout the time baseline of 2.3 times P_3. We note that the photographic and visual data between BJD 242 5000 and 243 3923 also show the cyclic signal. The poor fit prior to BJD 242 5000 may be due to the large errors and thus the low accuracy of the old photographic and visual data. Comparing the tortuous $O-C$ curve after BJD 242 5000, it is abnormal that the data prior to BJD 242 5000 have a time coverage of 41 yr, but show no variation. Considering the EW-type light curve of SW Lac (see fig. 1 in Pribulla et al. 1999), the errors of >0.01 d are possible for the old photographic and visual mid-eclipse times.

Our χ^2 contours of the solution (see Fig. 2) show that the orbital period of SW Lac D is less constrained by the 127 yr baseline, which is about 1.5 times P_4. We suspect that the outer and inner orbits are in a strict 3:1 MMR. So, the $O-C$ data are re-analysed using the LM method, but this time with the initial orbital periods of SW Lac D and C fixed at 3:1. The fitting process is iterated until the periods of both components result in a 3:1 ratio. The resonant parameters are listed in the last column (Solution 4) of Table 2. The strictly MMR fit is shown in Fig. 4, which is very similar to Fig. 1.

3 DYNAMICAL STUDY OF LTT MODEL

The solution constrains the orbital inclinations of both companions by $a_k \sin i_k$ ($k = 3, 4$) rather than uniquely determining them. We step through a series of i_3 sampled from 0° to 90°, and calculate the mass of the third body, m_3, with the mass function

$$f(m_3) = \frac{(m_3\sin i_3)^3}{(m_1+m_2+m_3)^2} = \frac{4\pi^2}{G{P_3}^2}\times(a_3\sin i_3)^3, \quad (8)$$

where m_1 and m_2 are the masses of the primary and secondary components, respectively. If the spectroscopic elements published by Ruciński et al. (2005) and the orbital inclination given by Ruciński, Pribulla & van Kerkwijk (2007, hereafter RPK07) are adopted, the combined mass of the binary pair $m_1 + m_2 = 2.13\,\mathrm{M}_\odot$. We also step i_4 from 0° to 180° and compute the mass of the fourth body, m_4, with

$$f(m_4) = \frac{(m_4\sin i_4)^3}{(m_1+m_2+m_3+m_4)^2} = \frac{4\pi^2}{G{P_4}^2}\times(a_4\sin i_4)^3. \quad (9)$$

The faint spectral signatures (Hendry & Mochnacki 1998; Ruciński et al. 2005) suggest that the companions are less massive. So, we assume $M_{3,4} < 5\,\mathrm{M}_\odot$, implying $i_{3,4} > 13.^\circ5$.

The mutually inclined angle between the inner and the outer orbits, φ, is determined by another angle, θ_4, which is the angle between the ascending node of SW Lac C and that of SW Lac D in the plane of the sky (see Fig. 5). θ_4 is stepped from 0° to 360°. Hence, we have to search the three-dimensional parameter space of (i_3, i_4, θ_4) (hereafter space I).

Then, we test the stabilities of all orbital configurations. The eclipsing binary pair is treated as a single object m_b with a mass equal to $m_1 + m_2 = 2.13\,\mathrm{M}_\odot$. Jacobian coordinates are used to describe the motion of the hierarchical triple system. The equations of the motion of three point-like masses (Harrington 1972) are

$$\ddot{\boldsymbol{r}}_{b3} = -G(m_b+m_3)\frac{\boldsymbol{r}_{b3}}{{r_{b3}}^3} - Gm_4\frac{\boldsymbol{r}_{b4}}{{r_{b4}}^3} + Gm_4\frac{\boldsymbol{r}_{34}}{{r_{34}}^3}$$

$$\ddot{\boldsymbol{r}}_{t4} = -G\frac{m_b+m_3+m_4}{m_b+m_3}\left[m_b\frac{\boldsymbol{r}_{b4}}{{r_{b4}}^3} + m_3\frac{\boldsymbol{r}_{34}}{{r_{34}}^3}\right], \quad (10)$$

where the vector $\boldsymbol{r}_{b3}$ refers to the Jacobian vector from m_b to m_3, and $\boldsymbol{r}_{t4}$ from the barycentre of the triple system (i.e. the eclipsing pair m_b and m_3, hereafter represented by the subscript 't') to m_4. In equations (10), the vector $\boldsymbol{r}_{b4} = \boldsymbol{r}_{t4} + m_3/(m_b+m_3)\boldsymbol{r}_{b3}$ denotes the position of m_4 relative to m_b, and $\boldsymbol{r}_{34} = \boldsymbol{r}_{t4} - m_b/(m_b+m_3)\boldsymbol{r}_{b3}$ is the position of m_4 relative to m_3. We choose the units of

Downloaded from https://academic.oup.com/mnras/article/439/1/878/1747721 by ANKARA user on 12 December 2021

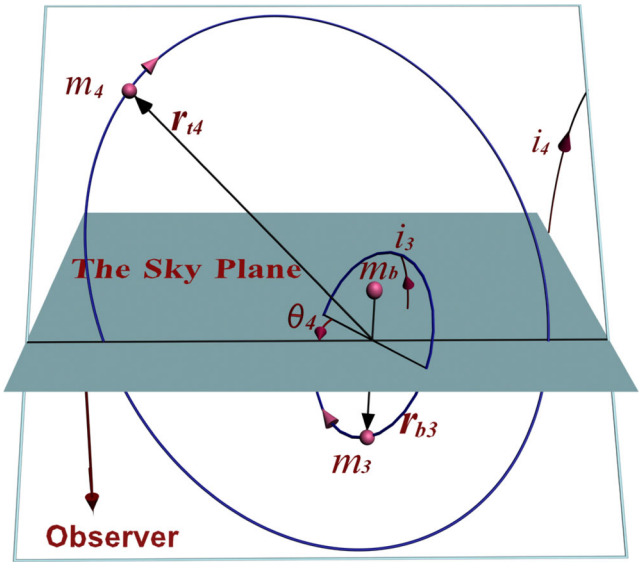


Figure 5. Schematic positions of the eclipsing binary and its two companions with respect to the tangent plane of the sky in Jacobian coordinates. m_b denotes the eclipsing pair, while m_3 and m_4 refer to its two companions.

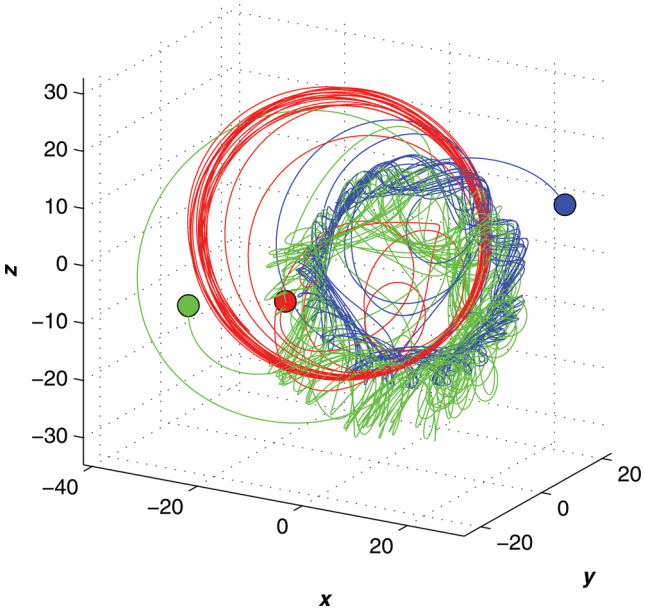


Figure 6. The evolution of one secularly pseudo-stable configuration ($i_3 = 42.^\circ9$, $i_4 = 76.^\circ9$, $\theta_4 = 32.^\circ1$) in the Cartesian coordinate system (x, y, z). The red, green and blue lines refer to the trajectories of SW Lac AB, C and D, respectively. The filled circles mark their original positions. The tangent plane of the sky is denoted by the x–y plane with the length unit of au. For clarity, only the trajectories on a 2000 year time-scale are plotted.

measurement to be au, yr and solar masses, so that the Newtonian gravitational constant is $G = 4\pi^2$.

In order to simulate the movements of two or more LTT bodies around one eclipsing binary, we develop a code called LTTBODIES, which is written in Intel Fortran for its support to the floating point data of 128 bit quadruple precision format. A 12(10) embedded Runge–Kutta–Nystrom algorithm with an adjustable time step (Dormand, El-Mikkawy & Prince 1987) is used in the code. We set a fractional error in position and velocity per step to about 10^{-12} during short-term integrations ($<10^3$ yr) and about 10^{-25} during long-term integrations ($>10^4$ yr), leading to a global error in the energy of $\sim10^{-10}$ for an integration time of 10^3 yr, and $\sim10^{-21}$ for 10^5 yr.

The initial conditions of our simulations are chosen as follows. First, the Keplerian orbits of the inner and outer pairs are derived from the best-fitting solution for one (i_3, i_4, θ_4) configuration. Throughout this paper, the near-MMR solution (Solution 2) is used as initial conditions, except that the MMR solution (Solution 4) is claimed explicitly. Note that the Jacobian orbits denoted by the subscripts of '$b3$' and '$t4$' are the same as the LTT orbits given by equation (2) (i.e. $e_{b3} = e_3$ and $e_{t4} = e_4$) except that (1) the semimajor axis $a_{b3} = a_3 \cdot (m_b + m_3)/m_3$ and $a_{t4} = a_4 \cdot (m_b + m_3 + m_4)/m_4$; (2) the argument of the periastron $\omega_{b3} = \omega_3 + \pi$ and $\omega_{t4} = \omega_4 + \pi$. In the second step, the latest mid-eclipse time (BJD time) is chosen as the starting time of the numerical integrations. The Jacobian position vectors of $\boldsymbol{r}_{b3,t4}$ and the velocity vectors of $\boldsymbol{v}_{b3,t4}$ at the time are calculated for the inner and outer pairs, respectively. In Section 3.3, $\boldsymbol{r}_{b3,t4}$ and $\boldsymbol{v}_{b3,t4}$ are changed slightly in the vicinity of their initial values derived in the second step.

3.1 Pseudo-stability

We perform a search in the space I in an equal interval of $0.^\circ2$. Out of ~600 million orbital configurations, several hundred can survive for $>10^4$ yr, one of which can survive for $>10^7$ yr (see Fig. 6). We also find that more configurations can survive for more longer times if smaller search grids are adopted. The mutual inclinations of these secularly stable configurations, φ, evolve from $58.^\circ4 \pm 24.^\circ6$ at the beginning to $126.^\circ0 \pm 36.^\circ0$ at 10^4 yr, and finally to $121.^\circ1 \pm 40.^\circ5$, where the formal uncertainties are obtained from their root-mean-square (rms) scatter. Interestingly, the sum of the mean values of φ before and after the long-term integrations is approximately 180°, by coincidence.

At the beginning of each numerical simulation, the secularly stable configuration changes rapidly from the best-fitting orbits to secularly stable, but very different ones. The best-fitting orbits, however, should be invariable on short time-scales of ~100 yr. So, these secularly stable configurations do not represent the true state of the SW Lac system.

3.2 Stability of the best-fitting orbits

To describe evolutionary deviations from the best-fitting orbits, we use two orbital parameters: the average distances and the average angular momenta. The relative amplitudes of the changes in the average orbital separations of the inner and outer pairs are defined respectively by

$$\delta_{b3} \equiv |\overline{r}_{b3} - \overline{r}_{b3,0}|/\overline{r}_{b3,0},$$

$$\delta_{t4} \equiv |\overline{r}_{t4} - \overline{r}_{t4,0}|/\overline{r}_{t4,0}, \quad (11)$$

where $\overline{r}_{b3}$ is the average value of r_{b3} in a time interval equal to P_3, and $\overline{r}_{b3,0}$ is the initial value of $\overline{r}_{b3}$. $\overline{r}_{b3,0}$ is computed as follows:

$$\overline{r}_{b3,0} = a_{b3}(1 + {e_{b3}}^2/2). \quad (12)$$

$\overline{r}_{t4}$ and $\overline{r}_{t4,0}$ are similar to $\overline{r}_{b3}$ and $\overline{r}_{b3,0}$, respectively.

The relative amplitudes of the momentum changes are defined by

$$\gamma_{b3} \equiv |\overline{L}_{b3} - L_{b3,0}|/|L_{b3,0}|,$$

$$\gamma_{t4} \equiv |\overline{L}_{t4} - L_{t4,0}|/|L_{t4,0}|, \quad (13)$$

Downloaded from https://academic.oup.com/mnras/article/439/1/878/1747721 by ANKARA user on 12 December 2021

where $\overline{L}_{b3,t4}$ are the average value of $L_{b3,\,t4}$ in a time interval equal to $P_{3,\,4}$, respectively. $L_{b3,\,t4}$ are the sizes of the angular momenta of the inner and outer pairs, respectively, determined by the following equations:

$$\boldsymbol{L}_{b3} = \frac{m_b m_3}{m_b + m_3}(\boldsymbol{r}_{b3} \times \dot{\boldsymbol{r}}_{b3}),$$

$$\boldsymbol{L}_{t4} = \frac{(m_b + m_3)m_4}{m_b + m_3 + m_4}(\boldsymbol{r}_{t4} \times \dot{\boldsymbol{r}}_{t4}). \quad (14)$$

In equations (13), $L_{b3,\,0}$ and $L_{t4,\,0}$ are the initial sizes of $\boldsymbol{L}_{b3}$ and $\boldsymbol{L}_{b3}$, respectively.

This time, the search in the space I is performed on a more dense grid size (i.e. 0.°1). In total, we compose ∼5 billion orbital configurations. The integration time is 320 yr. In such a short time-scale, the variations in average distances and average angular momenta should be at a low level. So, we assume

$$\delta_{b3,t4} < 0.1,$$

$$\gamma_{b3,t4} < 0.1. \quad (15)$$

The above assumptions are partly justified by the good fit of two-Keplerian orbits to the 127 year $O - C$ data of SW Lac (especially the photoelectric and CCD data in the latest 62 yr). In the past 127 yr, SW Lac C revolved several times in the orbit around AB (the eclipsing pair), with δ_{b3} and γ_{b3} both close to zero.

Furthermore, a hierarchical configuration is usually required for a stable multiple system (Perets & Fabrycky 2009), giving additional criteria:

$$a_{t4} > a_{b3},$$

$$\overline{r}_{t4} > \overline{r}_{b3}. \quad (16)$$

In this paper, we deem a configuration 'short-term stable' if it persists under the conditions given by equations (15) and (16) for a typical time-scale of 10^3 yr, and a configuration 'long-term stable' if no object escapes from the short-term stable system over a time-scale of $>10^4$ yr.

Out of ∼5 billion orbital configurations, 1155 configurations show such small-amplitude variabilities over the integration time of 320 yr, giving the smallest $\delta_{b3,\,t4}$ of 0.068 and 0.081, respectively. The locations of the 1155 configurations in the space I are plotted in the top panel of Fig. 7. It is obvious that the short-term stable configurations lie mainly along one straight line. i_3 ranges from 13.°9 to 90° and i_4 from 66° to 144°, giving that $m_3 > 0.62\,\mathrm{M}_\odot$ and $m_4 > 1.94\,\mathrm{M}_\odot$. As for θ_4, most points are in the interval 110°–140° with the remainder in 230°–240° and 270°–310°. The corresponding mutual inclinations of the inner orbit relative to the outer orbit φ ∼ 122.°2 with an rms of 4.°9, suggesting SW Lac D moves on a retrograde orbit with respect to SW Lac C. For instance, one of the 1155 configurations has the angular parameters of $i_3 = 69.°6$, $i_4 = 78.°1$ and $\theta_4 = 113.°4$, whose evolution is illustrated in Fig. 8. Furthermore, we find none of the 1155 configurations can maintain small-amplitude variabilities for 700 yr.

We also keep the initial orbits fixed at the MMR solution and search the space I in the same way as for the near-MMR solution. The short-term stable configurations are also plotted in the bottom panel of Fig. 7 and show similar distributions as in the top panel. The mutual inclinations $\varphi \sim 122.°2 \pm 6.°4$, coincident with the mean value in the near-MMR case. The 'lifetimes' of the short-term stable configurations are also less than ∼700 yr.

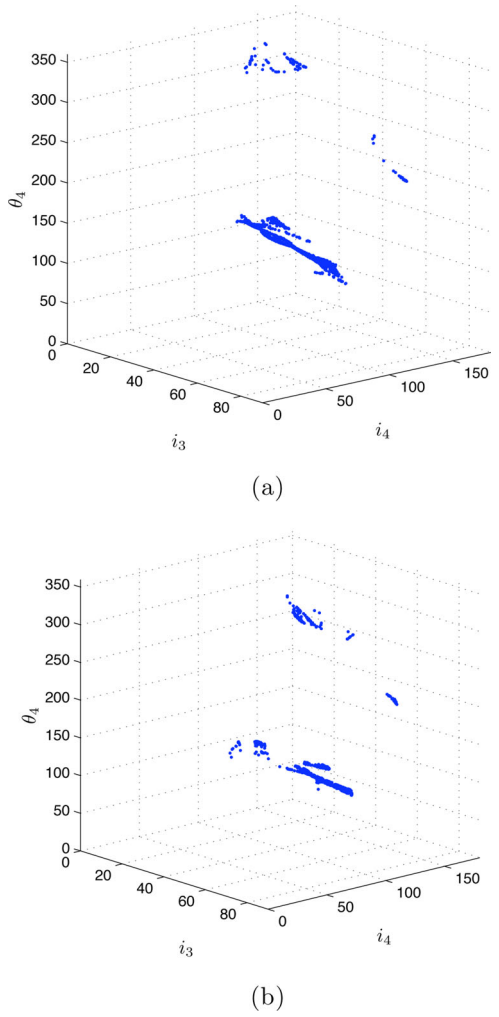


Figure 7. The distributions of the most stable systems on a 320 year time-scale for the near-MMR solution (a) and the MMR solution (b). Most points lie along one straight line in the three-dimensional parameter space of (i_3, i_4, θ_4).

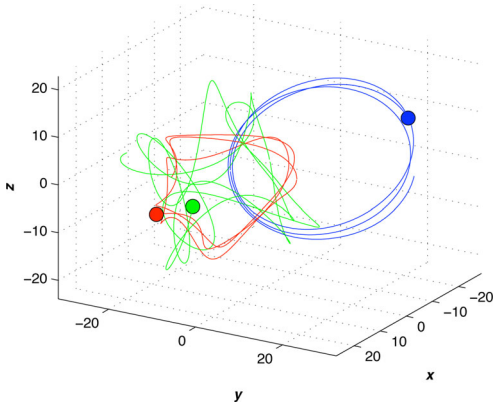


Figure 8. Same as Fig. 6, but for one short-term stable configuration ($i_3 = 69.°6$, $i_4 = 78.°1$, $\theta_4 = 113.°4$) on a 320 year time-scale.

3.3 Non-Keplerian corrections

Considering the shortcoming of the model of double-Keplerian orbits in describing the hierarchical system, we change $\boldsymbol{r}_{b3,t4}$ and

Downloaded from https://academic.oup.com/mnras/article/439/1/878/1747721 by ANKARA user on 12 December 2021

$\boldsymbol{v}_{b3,t4}$ slightly in the vicinity of their original values given by the double-Keplerian model. In the orbital plane of the inner pair, the projections of the Jacobian position vector $\boldsymbol{r}_{b3}$ and the velocity vector $\boldsymbol{v}_{b3}$ on to the direction parallel to the ascending node can be expressed as $\boldsymbol{r}_{b3//}$ and $\boldsymbol{v}_{b3//}$, respectively, and the projections on to the direction perpendicular to the ascending node as $\boldsymbol{r}_{b3\perp}$ and $\boldsymbol{v}_{b3\perp}$, respectively. Therefore, we have

$$\begin{aligned}\boldsymbol{r}_{b3} &= \boldsymbol{r}_{b3//} + \boldsymbol{r}_{b3\perp},\\ \boldsymbol{v}_{b3} &= \boldsymbol{v}_{b3//} + \boldsymbol{v}_{b3\perp}.\end{aligned} \tag{17}$$

Similarly,

$$\begin{aligned}\boldsymbol{r}_{t4} &= \boldsymbol{r}_{t4//} + \boldsymbol{r}_{t4\perp},\\ \boldsymbol{v}_{t4} &= \boldsymbol{v}_{t4//} + \boldsymbol{v}_{t4\perp}.\end{aligned} \tag{18}$$

We change the sizes of the parallel and perpendicular components of $\boldsymbol{r}_{b3,t4}$ and $\boldsymbol{v}_{b3,t4}$ simultaneously, but maintain the directions of eight components. For example, the size of $\boldsymbol{r}_{b3//}$ is varied from $r_{b3//} - 0.05\ r_{b3}$ to $r_{b3//} + 0.05\ r_{b3}$ in an equal interval of $0.01\ r_{b3}$, and so does the perpendicular component $\boldsymbol{r}_{b3\perp}$. New vector $\boldsymbol{r}_{b3}$ determined by its two modified components, together with other three new vectors, are taken as the initial conditions of our simulations. It is obvious that the eight-dimensional parameter space of ($\boldsymbol{r}_{b3//}$, $\boldsymbol{r}_{b3\perp}$, $\boldsymbol{v}_{b3//}$, $\boldsymbol{v}_{b3\perp}$, $\boldsymbol{r}_{t4//}$, $\boldsymbol{r}_{t4\perp}$, $\boldsymbol{v}_{t4//}$, $\boldsymbol{v}_{t4\perp}$)(hereafter space II) is open, but we only search the space near the point labelled by the original vectors $\boldsymbol{r}_{b3,t4}$ and $\boldsymbol{v}_{b3,t4}$.

For each of the 1155 short-term stable configurations, we hold the angles (i_3, i_4, θ) fixed and step through the space II with the relative deviations of ± 3 per cent from their initial values in an equal interval of 1 per cent, giving $7^8 = 5764\,801$ non-Keplerian initial conditions for each (i_3, i_4, θ_4) configuration. Over the integration time of, again, 320 yr, all 1155 configurations show the deviation of $\delta_{b3,\,t4} > 0.05$ and $\gamma_{b3,\,t4} > 0.05$ for all sets of non-Keplerian initial conditions.

4 THE VISUAL COMPANION

We note that a relatively distant companion (hereafter SW Lac E) is discovered around SW Lac AB in the adaptive optics search for circumbinary companions by RPK07. RPK07 found that the K5–M1 dwarf companion has a mass of $m_5 \sim 0.54\,\mathrm{M}_\odot$ and a sky-projected distance of $r_5 \sim 136$ au to SW Lac AB.

Since some essential orbital parameters are absent for SW Lac E, its orbit is assumed to be circular and determined by three independent parameters: the orbital inclination with respect to the sky plane, i_5, the angle between the ascending node of SW Lac C and that of SW Lac E, θ_5, and the argument of the fifth body measured from the ascending node in the sky plane, ω_5. The three parameters compose another space (hereafter space III).

As in the previous subsection, the 1155 short-term stable configurations in the space I are re-examined in the space III. The simulations are performed with the resolution of 1°. The inclusion of the fifth body, however, does not prolong their lives (say, 2000 yr). In particular, we find that the body exerts little influence on the orbit of the third and more influence on that of the fourth body. This is attributed to the larger value of r_5/r_{b3} than r_5/r_{t4}.

It is better to search the six-dimensional parameter space of (i_3, i_4, θ_4, i_5, ω_5, θ_5)(i.e. space I⊗III). Unfortunately, scanning the six-dimensional space is time consuming. We have to select arbitrarily the initial parameter $i_3 \in [14^\circ, 16^\circ, 30^\circ, 32^\circ, 60^\circ, 62^\circ]$ and search other five parameters (i_4, θ_4, i_5, ω_5, θ_5) with a resolution of 2°. Our scans also restrict ω_5 within the range of $0^\circ - 30^\circ$, based on the assumption of the circular orbit for SW Lac E. Once again, SW Lac E does not improve the dynamical stability of SW Lac C and D, giving the 'lifetime' less than 1000 yr. In addition, the stable configurations with $\delta_{b3,\,t4} < 0.1$ over a 320 year integration have similar angular distributions for SW Lac C and D, whether SW Lac E is considered or not. For instance, the short-term stable configurations with $i_3 = 32^\circ$ give $i_4 = 102\overset{\circ}{.}0 \pm 3\overset{\circ}{.}0$ and $\theta_4 = 128\overset{\circ}{.}4 \pm 2\overset{\circ}{.}4$ in the space I (SW Lac E is not considered) and $i_4 = 102\overset{\circ}{.}2 \pm 2\overset{\circ}{.}9$ and $\theta_4 = 128\overset{\circ}{.}3 \pm 2\overset{\circ}{.}5$ in the space I⊗III (SW Lac E is considered). Furthermore, $\delta_{b3,\,t4}$, in the presence of SW Lac E, can reach as small as 0.069 and 0.086, respectively, compared with 0.068 and 0.081 in the absence of SW Lac E.

5 DISCUSSIONS AND CONCLUSIONS

Based on our 11 mid-eclipse times together with the others collected from the literature, the $O - C$ diagram of SW Lac is plotted. The quadratic term (C_2) of equation (2) represents a continuous observed period increase with a rate of $\mathrm{d}P/\mathrm{d}t = 1.8 \times 10^{-7}\,\mathrm{d\,yr^{-1}}$. Given the period of the fifth body (i.e. SW Lac E) much longer than the baseline of the current data, the LTT effect contributed by the companion can be fitted by a quadratic term.

However, the increasing period may be partly attributed to mass transfer from the secondary component to the primary one. Assuming the conservation of mass, the maximum mass transfer rate can be estimated by the following equation (Singh & Chaubey 1986):

$$\frac{\dot{P}}{P} = \frac{3(1-q)}{q}\frac{\dot{m}_1}{m_2}, \tag{19}$$

where $q = m_2/m_1$ is the mass ratio of the eclipsing pair. Inserting $m_1 = 1.2\,\mathrm{M}_\odot$ and $q = 0.776$ into equation (19), the mass transfer rate $\mathrm{d}m_1/\mathrm{d}t = 6.0 \times 10^{-7}\,\mathrm{M}_\odot\,\mathrm{yr}^{-1}$.

The biperiodic variations of the $O - C$ curve provide evidence for two possible companions, which are closer to SW Lac than the one discovered by RPK07. The third and fourth bodies are in a near 3:1 MMR with periods of 27.01 and 82.61 yr, respectively. Based on the projected semimajor axes of the companions, the evolutions of the two inner companions in a series of orbital inclinations and mutual inclinations are simulated numerically in the absence of the fifth body. A series of simulations reveal that both of secularly pseudo-stable configurations and short-term invariable ones have the evolved mutual inclination of $\varphi \sim 116^\circ - 129^\circ$. Although the best-fitting parameters will be refined with high precision in the future, we believe that this result would hold since both of the MMR and near-MMR solutions give the same result. Horner et al. (2011) also proposed that significantly inclined orbits are more stable on an $\sim 10^4$ year time-scale.

The orbital inclinations of all short-term stable configurations show that SW Lac C and D are more massive than 0.62 and 1.94 $\mathrm{M}_\odot$, respectively. The faint spectral signatures discovered by Hendry & Mochnacki (1998) can be explained by SW Lac C and/or SW Lac E in terms of their low masses. As for the massive companion SW Lac D, its spectrum should be easily visible from spectroscopy as well as photometry. However, Ruciński et al. (2005) found a faint spectral contribution of about 1 per cent to the total light at 5184 Å spectral window. In addition, Pribulla et al. (1999) claimed that the possible third light is negligible in the light curve of SW Lac. It seems that SW Lac D does not exist, unless it is an unseen compact object (black hole or neutron star).

The formal errors on our best-fitting parameters are not used to calculate the initial conditions, but considered in another way, i.e. our detailed non-Keplerian scans around the best-fitting parameters.

Downloaded from https://academic.oup.com/mnras/article/439/1/878/1747721 by ANKARA user on 12 December 2021

On the other hand, the non-Keplerian scans can overcome the limits of fitting two static Keplerian orbits to a three-body system.

It reveals that the 'lifetime' of the two inner companions depends on the parameters of $\delta_{b3,t4}$ and $\gamma_{b3,t4}$. In general, the 'lifetimes' are shorter than ∼1000 yr, which is approximately equal to the orbital period of the fifth body (∼940 yr), suggesting that the short 'lifetime' of the two inner companions may be related to the outermost companion.

Then, SW Lac E is included in our simulations. But the system is yet highly unstable in a series of orbital configurations. We speculate that the whole system would survive for a longer time if the eccentricity of the fifth body is considered. Besides the known period P_5, an eccentric orbit is determined by other independent parameters: i_5, θ_5, ω_5 (the argument of the periastron measured from the ascending node), T_5 (the time of the periastron passage), a_5 (the sky-projected semimajor axis of the visual pair) and e_5 (eccentricity). Searching the six-parameter space is time consuming. Furthermore, in RPK07, the ∼136 au distance of the visual companion from SW Lac AB between 1998 and 2005 is not equal to the semi-axis of the visual pair. A precise projected semi-axis of $a_5 \cos i_5$ is difficult to be derived from the movement of the visual companion on the sky over such a short time baseline.

Fortunately, the distance of the outmost companion SW Lac E from SW Lac AB is an order of magnitude larger than those of the two inner companions, while the mass of SW Lac E is about one tenth of the total masses of SW Lac AB, C and D. In 320 yr, i.e. one third of orbital period of the outmost companion, the short-term influence of the outmost companion on the two inner companions is limited, and ignorable, which is confirmed by the similar results obtained in searching the spaces I and I⊗III. This is the reason why we integrate the orbital motion for only 320 yr in the absence of SW Lac E. We believe that our short-term simulations which neglect SW Lac E do make sense, and the corresponding results are valid, although it is important to keep in mind that the influence would be strong near the periastron if $e_5 > 0$.

If the variations in the observed eclipse times are due to the presence of circumbinary objects, the system should exhibit a short-term invariable and secularly stable configuration. But our exhaustive dynamical analyses show that the orbits of three companions are highly variable on time-scales of $<10^3$ yr. Furthermore, a series of non-Keplerian orbits of the two inner companions, with slight deviations from Keplerian orbits, are also dynamically unstable. Likewise, multiple circumbinary companions derived from the timing variations are found to be unstable for some other contact binaries, such as HU Aqr (Horner et al. 2011; Wittenmyer et al. 2012), SZ Her (Hinse et al. 2012), HW Vir (Horner et al. 2012), NN Ser (Funk et al. 2012), DP Leo (Funk et al. 2012) and QS Vir (Horner et al. 2013), although their companions are all planets or low-mass M-type dwarfs. We somewhat doubt the existence of SW Lac C and D. It is well known that SW Lac is magnetically active. It is possible that both circumbinary objects and the periodic magnetic activity (Applegate 1992; Yuan & Qian 2007) contribute to the timing variations. The only way to uncover the true nature is long-term observations in the future. Observed timing variations with strict periods are likely due to circumbinary object(s), while quasi-periodic variations are likely related to magnetic activity.

Finally, we stress that our failure to find the genuine stable system may be due to the large search grids and/or the scarcity of orbital parameters about the outmost companion and the weak constraint on the orbital period of the middle companion. If the spaces I, II and III are explored simultaneously, and the eccentricity of SW Lac E is considered, the whole system would survive for a longer time. Hence, more detailed and powerful computations and secular observations of this target are needed.

ACKNOWLEDGEMENTS

This work is supported by the Joint Fund of Astronomy of the National Natural Science Foundation of China (NSFC) and the Chinese Academy of Sciences (CAS) (Grant No. U1231121). We would like to thank Kreiner J. M. for his data base and an anonymous referee for some constructive suggestions about the fits to the $O-C$ data. We acknowledge Shanxi Normal University for providing computational resources and support that have contributed to the results reported within this paper.

REFERENCES

Al-Naimiy H. M. K., Al-Masharfeh T. H. SH., 2000, Ap&SS, 273, 83
Albayrak B., Gürol B., 2001, Inf. Bull. Var. Stars, 5069
Albayrak B., Djurašević G., Erkapić S., Tanriverdi T., 2004, A&A, 420, 1039
Alton K. B., Terrell D., 2006, J. Am. Assoc. Var. Star Obs., 34, 188
Applegate J. H., 1992, ApJ, 385, 621
Aslan Z., Asir A., Engin S., Tüfekcioglu Z., Yilmaz N., 1981, Inf. Bull. Var. Stars, 1908
Bookmyer B. B., 1965, AJ, 70, 133
Brát L., Zejda M., Svoboda P., 2007, Open Eur. J. Var. Stars, 74, 1
Broglia P., 1962, Mem. Soc. Astron. Italia, 33, 43
Brownlee R. R., 1957, ApJ, 125, 372
Chou K. C., 1963, AJ, 68, 342
Demircan O. et al., 1994, Inf. Bull. Var. Stars, 4126
Derekas A., Kiss L. L., Bebesi Zs., 2002, Inf. Bull. Var. Stars, 5255
Dormand J. R., El-Mikkawy M. E. A., Prince P. J., 1987, IMA J. Numer. Anal., 7, 423
Dugan R. S., Wright F. W., 1939, Contrib. Princenton Univ. Obs., 19, 17
Eastman J., Siverd R., Gaudi B. S., 2010, PASP, 122, 935
Essam A., Mahdy H. A., Hamdy M. A., 1992, Ap&SS, 188, 117
Evren S., Akan M. C., İbanoğlu C., 1985, Inf. Bull. Var. Stars, 2781
Faulkner D. R., Evans E. E., III, Grossoehme D. H., Moyer E. J., Jr, 1984, Inf. Bull. Var. Stars, 2473
Funk B., Eggl S., Gyergyovits M., Schwarz R., Pilat-Lohinger E., 2012, in Richards M. T., Hubenyeds I., eds, Proc. IAU Symp. 282, From Interacting Binaries to Exoplanets. Cambridge Univ. Press, Cambridge, p. 446
Harrington R. S., 1972, Celest. Mech., 6, 322
Hendry P. D., Mochnacki S. W., 1998, ApJ, 504, 978
Hinse T. C., Goździewsk K., Lee J. W., Haghighipour N., Lee C.-U., 2012, AJ, 144, 34
Hopp U., Hoffmann M., Witzigmann S., 1982, Inf. Bull. Var. Stars, 2142
Horner J., Marschall J. P., Wittenmyer R., Tinney C. G., 2011, MNRAS, 416, L11
Horner J., Hinse T. C., Wittenmyer R. A., Marshall J. P., Tinney C. G., 2012, MNRAS, 427, 2812
Horner J., Wittenmyer R. A., Hinse T. C., Marshall J. P., Mustill A. J., Tinney C. G., 2013, MNRAS, 435, 2033
Hübscher J., Paschke A., Walter F., 2006, Inf. Bull. Var. Stars, 5731
Hübscher J., Lehmann P. B., Monninger G., Steinbach H.-M., Walter F., 2010, Inf. Bull. Var. Stars, 5941
Irwin J. B., 1952, ApJ, 116, 211
Kalchaev K., Laytschev I. N., Trutse Yu. L., 1968, Var. Stars, 16, 440
Kılıçoğlu T. et al., 2007, Inf. Bull. Var. Stars, 5801
Kızılırmak A., Pohl E., 1974, Inf. Bull. Var. Stars, 937
Kreiner J. M., Kim C. H., Nha I. S., 2000, An Altas of O-C Diagrams of Eclipsing Binary Stars. Wydawnictwo Nauk. Akad. Pedagogicznej, Krakow, p. 2108
Kwee K. K., 1958, Bull. Astron. Inst. Neth. 14, 131
Lang K., Vetešník M., 1966, Bull. Astron. Inst. Czech., 17, 21

Downloaded from https://academic.oup.com/mnras/article/439/1/878/1747721 by ANKARA user on 12 December 2021

Markwardt C. B., 2009, in Bohlender D. A., Durand D., Dowler P., eds, ASP Conf. Ser. Vol. 411, Astronomical Data Analysis Software and Systems XVIII. Astron. Soc. Pac., San Francisco, p. 251
Mullis C. R., Faulkner D. R., 1991, Inf. Bull. Var. Stars, 3593
Muthsam H., Rakos K. D., 1974, A&AS, 13, 127
Müyesseroglu Z., Gürol B., Selam S. O., 1996, Inf. Bull. Var. Stars, 4380
Niarchos P. G., 1985, Inf. Bull. Var. Stars, 2820
Panchatsaram T., Abhyankar K. D., 1981, Bull. Astron. Soc. India., 9, 31
Perets H. B., Fabrycky D. C., 2009, ApJ, 697, 1048
Pohl E., 1967, Inf. Bull. Var. Stars, 198
Pohl E., Kızılırmak A., 1970, Inf. Bull. Var. Stars, 456
Pohl E., Kızılırmak A., 1972, Inf. Bull. Var. Stars, 647
Pohl E., Akan M. C., Ibanoğlu C., Sezer C., Güdür N., 1987, Inf. Bull. Var. Stars, 3078
Pribulla T., Chochol D., Parimucha Š., 1999, Contrib. Astron. Obs. Skalnaté Pleso, 29, 111
Ruciński S. M., 1968, Acta Astron., 18, 49
Ruciński S. M. et al., 2005, AJ, 130, 767
Ruciński S. M., Pribulla T., van Kerkwijk M. H., 2007, AJ, 134, 2353 (RPK07)
Singh M., Chaubey U. S., 1986, Ap&SS, 124, 389
Şenavcı H. V. et al., 2007, Inf. Bull. Var. Stars, 5754
Şenavcı H. V., Hussain G. A. J., O'Neal D., Barnes J. R., 2011, A&A, 529, 11
Widorn T., 1962, Mitt. Wien, 11, 1
Wittenmyer R. A., Horner J., Marshall J. P., Butters O. W., Tinney C. G., 2012, MNRAS, 419, 3258
Woodward E., 1951, AJ, 56, 77
Yuan J. Z., Qian S. B., 2007, ApJ, 669, L93
Zechmeister M., Kürster M., 2009, A&A, 496, 577
Zhai D. S., Lu W. X., 1989, Chin. Astron. Astrophys., 13, 350
Zhou A. Y., Jiang X. J., Zhang Y. P., Wei J. Y., 2009, Res. Astron. Astrophys., 9, 349

This paper has been typeset from a TEX/LATEX file prepared by the author.

Downloaded from https://academic.oup.com/mnras/article/439/1/878/1747721 by ANKARA user on 12 December 2021